PHYSICAL REVIEW B **96**, 241404(R) (2017)

Random-walk topological transition revealed via electron counting

G. Engelhardt,[1,2] M. Benito,[3,4] G. Platero,[3] G. Schaller,[1] and T. Brandes[1]

[1]*Institut für Theoretische Physik, Technische Universität Berlin, Hardenbergstr. 36, 10623 Berlin, Germany*

[2]*Beijing Computational Science Research Center, Beijing 100193, People's Republic of China*

[3]*Instituto de Ciencia de Material de Madrid, CSIC, 28049 Madrid, Spain*

[4]*Department of Physics, University of Konstanz, D-78457 Konstanz, Germany*

(Received 20 July 2017; revised manuscript received 6 October 2017; published 8 December 2017)

The appearance of topological effects in systems exhibiting a nontrivial topological band structure strongly relies on the coherent wave nature of the equations of motion. Here, we reveal topological dynamics in a classical stochastic random walk version of the Su-Schrieffer-Heeger model with no relation to coherent wave dynamics. We explain that the commonly used topological invariant in the momentum space translates into an invariant in a counting-field space. This invariant gives rise to clear signatures of the topological phase in an associated escape time distribution.

DOI: 10.1103/PhysRevB.96.241404

Introduction. Starting from topological insulators and superconductors [1–3], the manifestation of topological band structures has been investigated in various contexts. Relying on the wave nature of the dynamics, topological band structure effects also appear in bosonic and classical systems [4–11]. Furthermore, topological effects are manifested in quantum walk problems [12–19]. Thereby, a quantum mechanical particle moves randomly on a lattice, where the movement is determined by a quantum mechanical equation of motion. For this reason, the dynamics of the quantum walk inherits the wave nature of quantum mechanics which consequently can give rise to topological band structure effects.

In this Rapid Communication, we abandon the requirement of a wavelike motion and consider a purely stochastic random walk in a classical fashion. As we explain in the following, a properly designed system still exhibits clear features of a topological coupling geometry. We choose a random walk version of the celebrated Su-Schrieffer-Heeger (SSH) model to explain this effect. A sketch of the system is depicted in Fig. 1(a). The SSH model consists of a linear chain of nodes with staggered coupling strength and is presumably the simplest model exhibiting topological effects [20–22]. In our investigation, the state of the system can hop randomly along the SSH chain.

Due to the underlying topological coupling geometry, one can define a topological invariant (TI) based on the generalized density matrix, where the *counting field* takes the role of momentum in common topological band structures. We show that a properly defined escape time statistics will reveal the topology. Thereby, the SSH model with an open boundary condition is associated to the escape time from a finite region of the SSH random walk as depicted in Fig. 1(d).

Our approach requires a detailed counting statistics with a large number of experimental runs. In order to obtain the required amount of data, we suggest to implement the random walk using a single-electron transistor (SET), which in the full-counting space is described by a SSH random walk.

Understanding the relaxation dynamics of mesoscopic devices is of fundamental interest in the development of mesoscopic electronic devices [23,24] as single-electron emitters [25,26], quantum pumps [27–29], or solid state qubits [30]. A detailed counting statistics can provide information about the underlying processes and correlations arising in mesoscopic devices, as universal oscillations investigated in Refs. [31,32]. A basic theoretical knowledge is required to develop schemes to control the counting statistics [33,34]. In this regard, our findings contribute to the fundamental understanding of processes being active in such systems. The possibility of including feedback operations allows us to study even more sophisticated models [35].

The system. We consider a classical random walk on a one-dimensional lattice [Fig. 1(a)]. The sites are labeled by $n = 0, \pm 1, \pm 2, \ldots$. The random walk of the state $|n\rangle_t$ from time t to time $t + dt$ is determined by the transition probabilities p_+, p_-, p_s which are defined by

$$|n\rangle_t \to \begin{cases} |n+1\rangle_{t+dt} & \text{with} \quad p_+ = (\overline{\gamma} - (-1)^n \alpha) dt \\ |n-1\rangle_{t+dt} & \text{with} \quad p_- = (\overline{\gamma} + (-1)^n \alpha) dt \\ |n\rangle_{t+dt} & \text{with} \quad p_s = 1 - p_+ - p_-, \end{cases} \tag{1}$$

where $2\overline{\gamma} dt$ is the probability that the system escapes from site n within an infinitesimal time step dt. We impose a coupling geometry with an alternating hopping probability. The parameter α determines a jump bias so that for $\alpha \neq 0$ a jump to either $|n+1\rangle$ or $|n-1\rangle$ is preferred. The coupling geometry is thus analog to the SSH model [20,21]. Equation (1) appears in the transport dynamics of a SET, i.e., a quantum dot connected to two electronic leads, when the chemical potentials match the on-site energy of the quantum dot. In this case, the effective coupling parameters are $\Gamma_{\mathrm{L/R}} = \overline{\gamma} \pm \alpha$ (see Fig. 1(b) [35,36]).

For the following analysis, we introduce the parametrization $n = 2m - d$ with $m \in \mathbb{Z}$ and $d \in \{0,1\}$. The probability distribution corresponding to Eq. (1) follows the equation

$$\frac{d}{dt}\underline{\rho}_m = \mathbf{L}_0 \underline{\rho}_m + \mathbf{L}_+ \underline{\rho}_{m-1} + \mathbf{L}_- \underline{\rho}_{m+1}, \tag{2}$$

where $\underline{\rho}_m = (p_{m,1}, p_{m,0})^{\mathrm{T}}$ contains the probabilities $p_{m,d} = p_{n=2m-d}$ that the system is in state $|n = 2m - d\rangle$ and

$$\mathbf{L}_0 = \begin{pmatrix} -2\overline{\gamma} & \Gamma_{\mathrm{L}} \\ \Gamma_{\mathrm{L}} & -2\overline{\gamma} \end{pmatrix}, \mathbf{L}_+ = \begin{pmatrix} 0 & \Gamma_{\mathrm{R}} \\ 0 & 0 \end{pmatrix}, \mathbf{L}_- = (\mathbf{L}_+)^{\mathrm{T}}.$$

Regarding the SET [Fig. 1(b)], $\mathbf{L}_+$ describes a jump of an electron from the right reservoir into the dot, while the nondiagonal entries of $\mathbf{L}_0$ describe the jumps related to the left

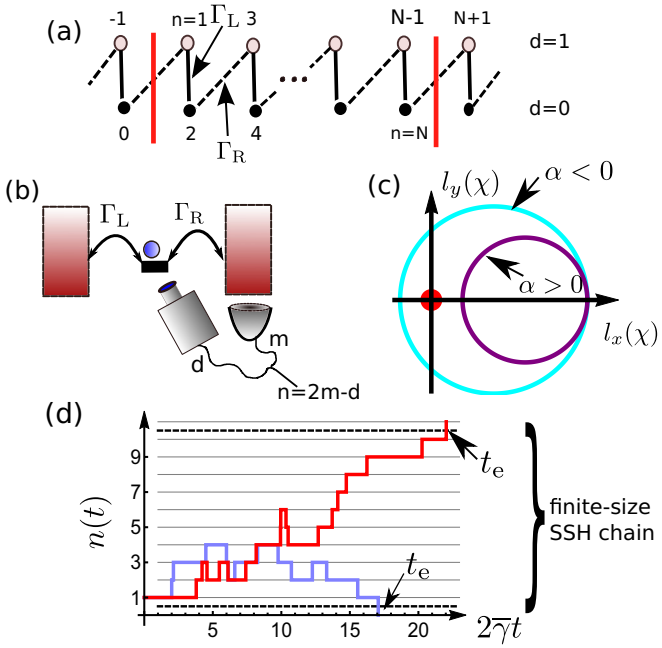

FIG. 1. (a) Stochastic random walk on a lattice with SSH coupling geometry. The state of the system $|n\rangle$ changes randomly as a function of time with alternating hopping probabilities according to Eq. (1). (b) This random walk describes the dynamics of a SET connected to two Markovian leads with properly adjusted chemical potentials, which are coupled to the dot with strengths Γ_R and Γ_L. By counting the number of particles tunneled into the right reservoir m and monitoring the dot occupation $d \in \{0,1\}$, one can infer the state $n = 2m - d$. (c) Illustration of the TI in the SSH model, which is equivalent to a winding of the curve $[l_x(\chi),l_y(\chi)]$ (depending on $\Gamma_{R/L}$) around the origin. (d) Stochastic trajectory of $|n\rangle_t$ as a function of time in units of $2\overline{\gamma} = \Gamma_R + \Gamma_L$. At time t_e the state escapes from the region $\{1,...,N\}$, resembling the quantum SSH model with an open boundary condition.

reservoir. Additionally, the diagonal terms $-2\overline{\gamma} = -\Gamma_L - \Gamma_R$ are responsible for the correct normalization of the probability distribution $\sum_n p_n = 1$. The index m can thus be interpreted as the number of particles having jumped out of the right reservoir. For instance, if the initial state is $p_n(0) = \delta_{n,1}$, then we have one particle $m = 1$ tunneled out of the right reservoir and a dot occupation of $d = 1$.

Relation to the Schrödinger equation and topology. By replacing $d/dt \to \mathrm{i}d/dt$, Eq. (2) becomes equivalent to the Schrödinger equation of a particle in the quantum mechanical SSH model, when interpreting $\underline{\rho}_m$ as the corresponding wave function. We emphasize that the introduction of the complex unit i is more than a reparametrization, but renders one real-valued equation into a complex-valued (thus, two real-valued) equation(s). As a consequence, we obtain the wavelike Schrödinger equation, so that we can expect different kinds of physical dynamics.

Yet, the formal analogy to the quantum SSH Hamiltonian gives rise to topological effects in a stochastic random walk. To see this, we apply the concepts known from the quantum model to introduce a TI.

By applying a Fourier transformation Eq. (2) becomes

$$\dot{\underline{\rho}}(t,\chi) = \mathbf{L}_\chi\, \underline{\rho}(t,\chi), \qquad \mathbf{L}_\chi = -2\overline{\gamma}\mathbf{1} + \underline{l}(\chi)\cdot\underline{\boldsymbol{\sigma}}, \tag{3}$$

where $\underline{l}(\chi) = [l_x(\chi),l_y(\chi)]$ with $l_x(\chi) = \Gamma_L + \Gamma_R\cos(\chi)$, $l_y(\chi) = \Gamma_R\sin(\chi)$ and $\underline{\boldsymbol{\sigma}} = [\boldsymbol{\sigma}_x,\boldsymbol{\sigma}_y]$ with $\boldsymbol{\sigma}_{x,y,z}$ denote the usual Pauli matrices. Importantly, $(1,1)\cdot\underline{\rho}(t,\chi)$ represents the moment generating function, whose derivatives with respect to χ are the moments of the probability distribution $p_m(t)$ that the system is in either the state $n = 2m$ or $n = 2m - 1$.

The matrix $\mathbf{L}_\chi$ is equivalent to the matrix representation of the SSH Hamiltonian in momentum space when identifying the counting field χ with the momentum. In particular, we can define two topological phases for $\alpha > 0$ (trivial) and $\alpha < 0$ (nontrivial) which are characterized by a TI: $2\pi W = \int_{-\pi}^{\pi} d\chi\, \frac{d}{d\chi}\arg[l_y(\chi)/l_x(\chi)]$, which is $W = 0$ (trivial) or $W = 1$ (nontrivial). This invariant is equal to the winding of the curve $\underline{l}(\chi)$ around the origin as illustrated in Fig. 1(c). We note that W is also directly linked to the geometrical Berry (or Zak) phase $\phi_{\mathrm{Berry}} = W/2$ [37]. Importantly, the definition of an invariant requires that there is no term proportional to $\boldsymbol{\sigma}_z$ appearing in Eq. (3). This is guaranteed by the existence of a *chiral* symmetry in the equations of motion [3,21]. For our system Eq. (1) this means that the probability to escape from the even and odd sites n is equal [38].

The strict quantization of W in an infinite-size system has a strict consequence for the finite-size (quantum) SSH Hamiltonian defined on the sites $n \in \{1,\ldots,N\}$ with an open boundary condition [21], i.e., with zero coupling between $n = 0$, $n = 1$ and $n = N$, $n = N + 1$. The corresponding spectrum exhibits topologically protected *midgap modes* if the system is in the nontrivial phase. We depict such spectra in Fig. 2 with orange solid lines for different chain lengths N. The symmetry around $E = -2\overline{\gamma}$ of the spectrum is a consequence of the chiral symmetry. In Figs. 2(a) and 2(b) we depict the spectrum for an even number of sites N. We find a pair of energies for $\alpha > 0$ at the inner boundaries of the bands which merge for decreasing α and become degenerate for $\alpha \lesssim 0$. This is a typical signature in the nontrivial phase of the SSH model. Due to the inversion symmetry in the SSH chain for N even, the wave function of these two midgap states at $E = -2\overline{\gamma}$ are symmetric and antisymmetric upon inversion, respectively [21]. For N odd the chain also exhibits a generalized inversion symmetry [35]. The corresponding spectrum is depicted in Fig. 2(c). We observe for all α a midgap state, whose wave function is localized close to $n = 1$ ($n = N$) for $\alpha < 0$ ($\alpha > 0$).

Escape time distribution. The TI described by W is a theoretical classification of the topological phase which can be hardly determined in experiment. However, the close analogy to the SSH model and the localized midgap modes allow for a different detection scheme.

To this end, we use the existence or absence of midgap modes in a finite-size system. We construct an associated escape time distribution (ETD), which resembles an open boundary condition of the quantum SSH model: We divide the originally infinite chain in Fig. 1(a) in three parts. The middle section consisting of sites $n \in \{1,\ldots,N\}$ constitutes the random walk analog of the SSH model with an open boundary condition: Defining the probability vector $\underline{\rho} = (p_{n=1},\ldots,p_{n=N})$ containing the probabilities of the middle section, we can represent Eq. (2) as

$$\dot{\underline{\rho}} = \mathbf{L}_{\mathrm{SSH}}\underline{\rho} + \underline{J}_1 p_0 + \underline{J}_N p_{N+1}, \tag{4}$$

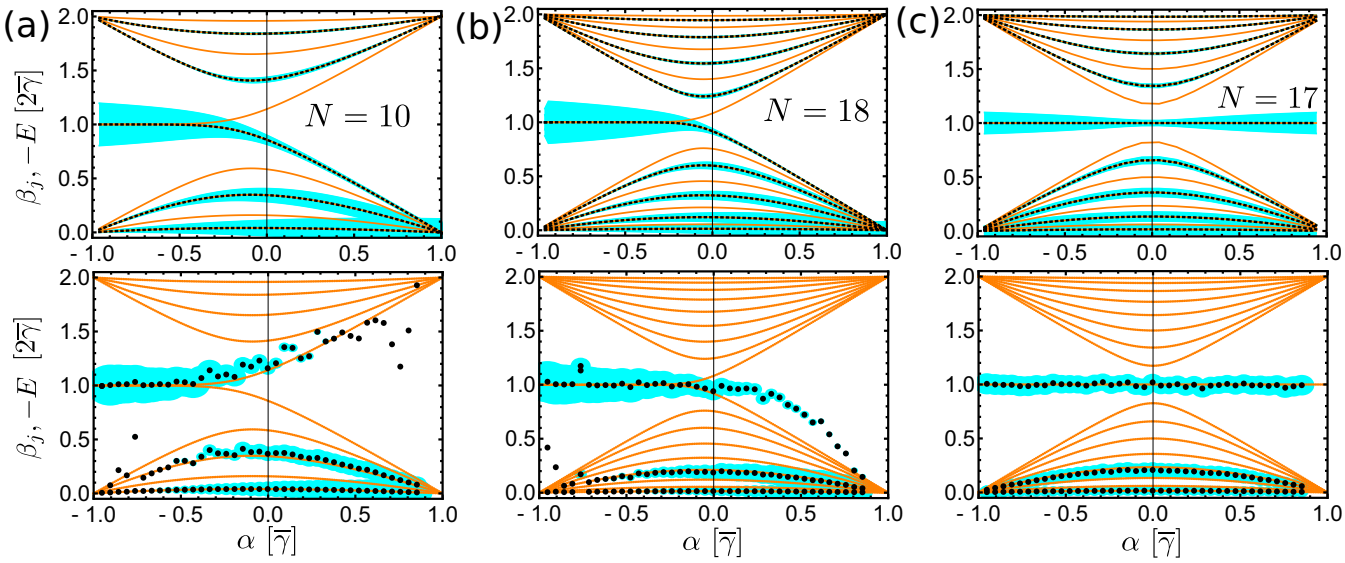

FIG. 2. Comparison of the spectrum of $\mathbf{L}_{\mathrm{SSH}}$ in Eq. (4) with open boundary conditions and the exponent spectrum β_i of the integrated ETD according to Eq. (6). In (a), (b), and (c) we depict the results for the chain lengths $N = 10$, $N = 18$, and $N = 17$, respectively. The orange (solid) lines depict the spectrum of the matrix $\mathbf{L}_{\mathrm{SSH}}$. The top panels depict the exact results obtained by a diagonalization. The dotted exponent spectrum depicts the levels with nonvanishing coefficients A_j [see Eq. (6)]. The coefficients A_j are represented by the blue regions, whose width is proportional to A_j. The bottom panels depict the exponent spectrum obtained by a simulation of random trajectories. To construct the integrated ETD we used $i_{\max} = 10^5$ random trajectories, which have been fitted with $K = 3$.

where the entries of the *jump vectors* read $(\underline{J}_1)_k = \Gamma_{\mathrm{R}}\delta_{1,k}$ and $(\underline{J}_N)_k = [\overline{\gamma} - (-1)^N\alpha]\delta_{N,k}$. Importantly, $\mathbf{L}_{\mathrm{SSH}}$ is equivalent to the quantum SSH Hamiltonian with an open boundary condition. We investigate the time t_{e} at which the state escapes from the finite-size SSH section when initiated at a SSH site at $t_0 = 0$. This means that the experimentalist creates the open boundary condition by stopping the experimental run when the state leaves the finite-size SSH section which is feasible with current experimental technologies [33].

The probability that the system escapes from the SSH chain at time t_{e} reads [35,39]

$$P_{\mathrm{e}}(t_{\mathrm{e}}) = \underline{J}^T e^{\mathbf{L}_{\mathrm{SSH}}t_{\mathrm{e}}}\underline{\rho}(0) = \sum_{j=1}^{K} a_j e^{-\beta_j t_{\mathrm{e}}} > 0, \qquad (5)$$

where $\underline{J}^{\mathrm{T}}$ is the transpose of $\underline{J} = \underline{J}_1 + \underline{J}_N$. For the second equality we have used the eigenvalues $E_j = -\beta_j$ and eigenstates $\underline{v}_j$ of $\mathbf{L}_{\mathrm{SSH}}$. The coefficients read $a_j = (\underline{J}^{\mathrm{T}} \cdot \underline{v}_j)(\underline{v}_j^{\mathrm{T}} \cdot \underline{\rho}(0))$ and $K = N$. The time dependence of the ETD is thus determined by the eigenstates and eigenvalues of the finite-size SSH model, and consequently, of the underlying topology. The integrated ETD

$$P_{\mathrm{int}}(t) = \int_0^t P_{\mathbf{e}}(t')dt' = 1 - \sum_{j=1}^{j=K} A_j e^{-\beta_j t} \qquad (6)$$

fulfills $P_{\mathrm{int}}(\infty) = 1$. From Eq. (6) we find that $\sum_j A_j = 1$ and $A_j = -a_j/\beta_j$.

In the following, we choose a symmetric initial state $p_n(t = 0) = \delta_{n,1}/2 + \delta_{n,N}/2$. An example of the resulting ETD is depicted in Fig. 3(a) with a solid line, which shows its decaying character. Even though there is an underlying but complex relation between the exponent spectrum and the cumulants [40], the moments $\mu_m = \int_0^\infty t^m P_{\mathbf{e}}(t)dt$ and the associated cumulants κ_m [41] depicted in Fig. 3(b) do not provide direct information about the topology.

For this reason, we continue to investigate the exponents β_j and coefficients A_j determining the integrated ETD. These are depicted in the top row of Fig. 2. The β_j for nonvanishing A_j are depicted with black (dotted) lines and their coefficients A_j are represented by the blue regions, whose width is proportional to A_j. Importantly, in Fig. 2 we can only find every second β_j. This is related to the (generalized) inversion symmetry of the system. For N even, the eigenstates $\underline{v}_j$ exhibit either even ($v_{j,n} = v_{j,N+1-n}$) or odd ($v_{j,n} = -v_{j,N+1-n}$) parity. Therefore, the coefficients a_j and A_j for the odd eigenstates vanish as $\underline{J}$ has even parity, $(\underline{J})_n = (\underline{J})_{N+1-n}$. A

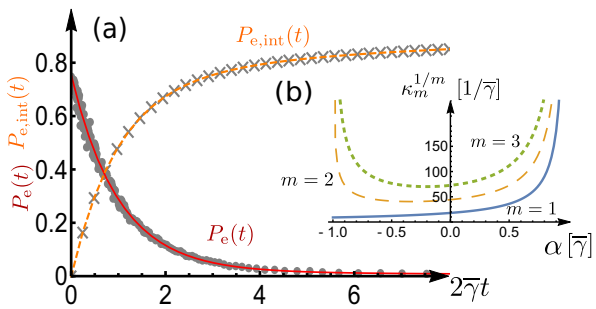

FIG. 3. (a) depicts the reconstructed escape time distribution (ETD) $P_{\mathrm{e}}(t)$ (dots), the reconstructed integrated ETD $P_{\mathrm{e,int}}(t)$ (crosses), and the corresponding fitted curves with solid and dashed lines for $\alpha = -0.5\overline{\gamma}$. (b) Cumulants κ_m of the ETD for $m = 1$ (solid), $m = 2$ (dashed), and $m = 3$ (dotted) as a function of α. The depicted and higher cumulants do not reveal any signature of topology as, e.g., a nonanalyticity at $\alpha = 0$.

similar reasoning applies for N odd [35]. Remarkably, the coefficients of the midgap modes for $N = 10$ and $N = 18$ are very similar. This is a consequence of the fact that the midgap eigenvectors only slightly depend on the system size. Due to the symmetric initial condition $\underline{\rho}(0)$, we find also symmetric coefficients A_j with respect to $\alpha \to -\alpha$ for $N = 17$.

Detection of the topological phase. After investigating the dynamics on the probability level, we now return to the random walk according to Eq. (1). We can reconstruct the ETD by initializing the system on a site n and measuring the escape time t_e [Fig. 1(d)]. By repeatedly conducting this experiment and determining the escape times $t_{e,i}$, with $i = 1, \ldots, i_{\max}$ we can construct the ETD and the integrated ETD [35]. To resemble the initial state $p_n(t = 0) = \delta_{n,1}/2 + \delta_{n,N}/2$, we start half of the random trajectories on site $n = 1$ and the other half on site $n = N$. In Fig. 3(a), we depict the reconstructed distributions for $\alpha = -0.5\overline{\gamma}$ by using $i_{\max} = 10^5$ random trajectories.

Fitting the reconstructed ETD with the ansatz Eq. (5) provides information about the eigenvalues of $\mathbf{L}_{\mathrm{SSH}}$. We use the integrated ETD and Eq. (6) instead of the ETD as this provides a higher degree of reliance for the fit parameters, in particular for small β_j. We find that in Eq. (6) $K = 3$ is sufficient to resemble the reconstructed integrated ETD with a high accuracy. The case $K > 3$ is discussed in Ref. [35]. In the bottom row of Fig. 2, we depict the exponent spectrum $\{\beta_j\}$ obtained with this procedure.

For a short chain length $N = 10$, the exponent spectrum agrees well with the spectrum of $\mathbf{L}_{\mathrm{SSH}}$ for $\beta_j \lesssim 2\overline{\gamma}$. In particular, the midgap state with $\beta_j = 1$ is clearly visible in the nontrivial phase for $\alpha < 0$. The eigenstates with $\beta_j > 2\overline{\gamma}$ are not resembled by this procedure. This is a consequence of the corresponding small A_j in the expansion Eq. (6) and the fast transition dynamics related to the relative large β_j. Remarkably, the fitting procedure resembles every second eigenvalue for $\beta_j < 2\overline{\gamma}$. Thus, we observe the eigenvalues with even parity according to our previous explanation and according to the top panel in Fig. 2(a). Moreover, corresponding to the theoretical prediction the fitted A_j are considerably larger for the midgap state as for the other β_j. For $\alpha > 0$ we find some β_j which do not fit to the spectrum of $\mathbf{L}_{\mathrm{SSH}}$. However, the corresponding A_j are small so that they do not significantly influence the fit quality.

For a longer chain with $N = 18$ we observe similar features. In particular, we also recognize the midgap state. For $N = 17$, the exponent spectrum of the reconstructed integrated ETD resembles the main features of the $\mathbf{L}_{\mathrm{SSH}}$ spectrum. Due to the chosen initial condition, the coefficients A_j are equal for α and $-\alpha$. This results in the symmetry observed in Fig. 2(c), where the midgap exponents are located at $\beta_j \approx 2\overline{\gamma}$ for all α values.

Conclusions. We showed that a classical random walk on a lattice with SSH coupling geometry exhibits a TI signaling the topological phase. This TI is defined by the generalized density matrix as a function of the counting field χ, which constitutes the analog description of the system in momentum space known from the quantum SSH model. This relation is reminiscent but distinct from the investigations Refs. [42–47] establishing also a link between counting statistics and topology. We showed that the topological phase is revealed in the spectrum of fitted exponents of a properly designed ETD. Although the fitting procedure applied to the random data is sensitive to numerical details, we found that boundary modes are strongly pronounced in the exponent spectrum. This feature remains independent of the chain length, which confirms the underlying topological character in the stochastic dynamics. Even for moderately time-fluctuating rates, which keep the chiral symmetry $\Gamma_{\mathrm{L}}(t) + \Gamma_{\mathrm{R}}(t) = \overline{\gamma}$, the presence or absence of the midgap mode should not be changed. Moreover, even for a next-nearest neighbor hopping (e.g., caused by missing a jump due to a finite detector time resolution), a topological classification is possible if there is still a chiral symmetry. These exponents provide thus a characterization of the ETD different from the cumulants, which do not exhibit direct information about the topology.

The required experimental data can be generated using quantum dots with an adjacent quantum point contact [31]. This amount of data is in the order of magnitude needed to detect the topological dynamics. In order to enable a bidirectional particle counting required for our proposal, one could harness an experimental setup as in Refs. [48,49]. There the direction of a particle jump (into the reservoirs or out from the reservoir) can be detected by a spatial bipartition of the quantum dot and an asymmetrically coupled quantum point contact.

To resemble the SSH dynamics and topological issues, we considered here specially chosen chemical potentials. However, even for a general temperature and voltage bias, the generalized master equation can exhibit fascinating (topological) effects such as exceptional points [50]. A similar escape time experiment could in this case reveal the underlying physical processes. Moreover, the suggested setup can be harnessed to create more complex random walks by means of feedback control as we discuss in Ref. [35].

The discovered topology in random walks is not restricted to nanoelectronic devices as the SET but can appear in other kinds of random walk setups. In this respect it will be interesting to consider extensions to two or higher dimensional random walk lattices.

The authors gratefully acknowledge financial support from the DFG Grants No. BR 1528/9-1 and No. SFB 910. This work was financially supported by the Spanish Ministry through Grant No. MAT2014-58241-P, the FPI program, and the National Natural Science Foundation of China (under Grant No. U1530401).

[1] M. Z. Hasan and C. L. Kane, Rev. Mod. Phys. **82**, 3045 (2010).

[2] B. A. Bernevig and T. L. Hughes, *Topological Insulators and Topological Superconductors* (Princeton University Press, Princeton, 2013).

[3] C.-K. Chiu, J. C. Y. Teo, A. P. Schnyder, and S. Ryu, Rev. Mod. Phys. **88**, 035005 (2016).

[4] G. Engelhardt and T. Brandes, Phys. Rev. A **91**, 053621 (2015).

[5] G. Engelhardt, M. Benito, G. Platero, and T. Brandes, Phys. Rev. Lett. **117**, 045302 (2016).

[6] G. Engelhardt, M. Benito, G. Platero, and T. Brandes, Phys. Rev. Lett. **118**, 197702 (2017).
[7] V. Peano, M. Houde, F. Marquardt, and A. A. Clerk, Phys. Rev. X **6**, 041026 (2016).
[8] R. Süsstrunk and S. D. Huber, Science **349**, 47 (2015).
[9] C. Poli, M. Bellec, U. Kuhl, F. Mortessagne, and H. Schomerus, Nat. Commun. **6**, 6710 (2015).
[10] C. H. Lee, G. Li, G. Jin, Y. Liu, and X. Zhang, arXiv:1701.03385.
[11] M. Bello, C. Creffield, and G. Platero, Sci. Rep. **6**, 22562 (2016).
[12] V. V. Ramasesh, E. Flurin, M. Rudner, I. Siddiqi, and N. Y. Yao, Phys. Rev. Lett. **118**, 130501 (2017).
[13] E. Flurin, V. V. Ramasesh, S. Hacohen-Gourgy, L. S. Martin, N. Y. Yao, and I. Siddiqi, Phys. Rev. X **7**, 031023 (2017).
[14] P. M. Preiss, R. Ma, M. E. Tai, A. Lukin, M. Rispoli, P. Zupancic, Y. Lahini, R. Islam, and M. Greiner, Science **347**, 1229 (2015).
[15] J. Kempe, Contemp. Phys. **44**, 307 (2003).
[16] J. K. Asbóth and H. Obuse, Phys. Rev. B **88**, 121406 (2013).
[17] J. K. Asbóth, Phys. Rev. B **86**, 195414 (2012).
[18] T. Kitagawa, M. S. Rudner, E. Berg, and E. Demler, Phys. Rev. A **82**, 033429 (2010).
[19] T. Kitagawa, M. A. Broome, A. Fedrizzi, M. S. Rudner, E. Berg, I. Kassal, A. Aspuru-Guzik, E. Demler, and A. G. White, Nat. Commun. **3**, 882 (2012).
[20] W. P. Su, J. R. Schrieffer, and A. J. Heeger, Phys. Rev. Lett. **42**, 1698 (1979).
[21] J. K. Asbóth, L. Oroszlány, and A. Pályi, in *Lecture Notes in Physics* (Springer, Berlin, 2016), Vol. 919.
[22] A. Gómez-León and G. Platero, Phys. Rev. Lett. **110**, 200403 (2013).
[23] J. Schulenborg, R. B. Saptsov, F. Haupt, J. Splettstoesser, and M. R. Wegewijs, Phys. Rev. B **93**, 081411 (2016).
[24] J. Schulenborg, J. Splettstoesser, M. Governale, and L. D. Contreras-Pulido, Phys. Rev. B **89**, 195305 (2014).
[25] G. Fève, A. Mahe, J.-M. Berroir, T. Kontos, B. Placais, D. Glattli, A. Cavanna, B. Etienne, and Y. Jin, Science **316**, 1169 (2007).
[26] M. Blumenthal, B. Kaestner, L. Li, S. Giblin, T. Janssen, M. Pepper, D. Anderson, G. Jones, and D. Ritchie, Nat. Phys. **3**, 343 (2007).
[27] M. R. Buitelaar, V. Kashcheyevs, P. J. Leek, V. I. Talyanskii, C. G. Smith, D. Anderson, G. A. C. Jones, J. Wei, and D. H. Cobden, Phys. Rev. Lett. **101**, 126803 (2008).
[28] F. Giazotto, P. Spathis, S. Roddaro, S. Biswas, F. Taddei, M. Governale, and L. Sorba, Nat. Phys. **7**, 857 (2011).
[29] J. Splettstoesser, M. Governale, J. König, and R. Fazio, Phys. Rev. Lett. **95**, 246803 (2005).
[30] R. Hanson, B. Witkamp, L. M. K. Vandersypen, L. H. Willems van Beveren, J. M. Elzerman, and L. P. Kouwenhoven, Phys. Rev. Lett. **91**, 196802 (2003).
[31] C. Flindt, C. Fricke, F. Hohls, T. Novotný, K. Netočný, T. Brandes, and R. J. Haug, Proc. Natl. Acad. Sci. USA **106**, 10116 (2009).
[32] K. Ptaszyński, Phys. Rev. B **96**, 035409 (2017).
[33] T. Wagner, P. Strasberg, J. C. Bayer, E. P. Rugeramigabo, T. Brandes, and R. J. Haug, Nat. Nanotechnol. **12**, 218 (2017).
[34] T. Brandes, Phys. Status Solidi B **254**, 1600548 (2017).
[35] See Supplemental Material at http://link.aps.org/supplemental/10.1103/PhysRevB.96.241404 for more details concerning this point.
[36] E. Bonet, M. M. Deshmukh, and D. C. Ralph, Phys. Rev. B **65**, 045317 (2002).
[37] M. V. Berry, Proc. R. Soc. London A **392**, 45 (1984).
[38] In general, a Hermitian matrix $\mathbf{L}$ exhibits chiral symmetry if there is a $x \in \mathbb{R}$ and a unitary Hermitian matrix $\mathbf{\Sigma}$ so that $\mathbf{\Sigma}(\mathbf{L} - x)\mathbf{\Sigma} = -(\mathbf{L} - x)$. As a result, the spectrum is symmetric about x. Here, we identify $\mathbf{\Sigma} = \boldsymbol{\sigma}_z$ and $x = -2\overline{\gamma}$.
[39] T. Brandes, Ann. Phys. (Berlin) **17**, 477 (2008).
[40] P. Stegmann and J. König, New J. Phys. **19**, 023018 (2017).
[41] G. Schaller, *Open Quantum Systems Far from Equilibrium* (Springer, New York, 2014), Vol. 881.
[42] C. Wang, J. Ren, and J. Cao, Phys. Rev. A **95**, 023610 (2017).
[43] J. Ren, P. Hänggi, and B. Li, Phys. Rev. Lett. **104**, 170601 (2010).
[44] F. Li, J. Ren, and N. A. Sinitsyn, EPL (Europhys. Lett.) **105**, 27001 (2014).
[45] J. Ren and N. A. Sinitsyn, Phys. Rev. E **87**, 050101 (2013).
[46] M. Benito, M. Niklas, G. Platero, and S. Kohler, Phys. Rev. B **93**, 115432 (2016).
[47] N. A. Sinitsyn and I. Nemenman, EPL **77**, 58001 (2007).
[48] Y. Utsumi, D. S. Golubev, M. Marthaler, K. Saito, T. Fujisawa, and G. Schön, Phys. Rev. B **81**, 125331 (2010).
[49] T. Fujisawa, T. Hayashi, R. Tomita, and Y. Hirayama, Science **312**, 1634 (2006).
[50] S. Daryanoosh, H. M. Wiseman, and T. Brandes, Phys. Rev. B **93**, 085127 (2016).